NANO LETTERS

2006
Vol. 6, No. 8
1645−1649

$Na(Y_{1.5}Na_{0.5})F_6$ Single-Crystal Nanorods as Multicolor Luminescent Materials

Leyu Wang[†,‡] and Yadong Li[*,†,‡]

Department of Chemistry, Tsinghua University, Beijing, 100084, P R China, and Anhui Key Laboratory of Functional Molecular Solids, College of Chemistry and Materials Science, Anhui Normal University, Wuhu, 241000, P R China

Received March 27, 2006; Revised Manuscript Received June 21, 2006

ABSTRACT

A facile wet chemical synthesis method was used to prepare a range of single-crystal $Na(Y_{1.5}Na_{0.5})F_6$ nanorods with controllable aspect ratios. Their novel multicolor upconversion (UC) fluorescence has been successfully realized by doping Yb^{3+}/Er^{3+} (green) and Yb^{3+}/Tm^{3+} (blue) ion pairs. When doped with Eu^{3+} and Tb^{3+} ions, the strong red and green downconversion (DC) fluorescence has also been observed, respectively. Being covered with oleic acids, these luminescent nanorods have been transparently dispersed in nonpolar solvent. For their unique luminescence and controllable morphology and surface properties, these nanorods may find great applications in the fields of color displays, biolabels, light-emitting diodes (LEDs), optical storage, optoelectronics, anticounterfeiting, and solid-state lasers.

Because of their size- and shape-dependent properties, single-crystal one-dimensional (1D) nanostructures have been identified as critical building blocks for nanoscale optoelectronics,[1−3] waveguide,[4] electronics,[5−8] lasers,[1,9,10] solar cells,[11−13] and gas and biochemical sensors.[14−17] However, among the researched 1D luminescent nanomaterials, significant efforts have been mainly based on the band-edge emission in semiconductor nanostructures.[9,12,18−23] Lanthanide (e.g., Yb^{3+}/Er^{3+}, Yb^{3+}/Tm^{3+}, etc.)-doped materials possess novel upconversion (UC) fluorescence properties, whose growth might promise great potentials for UC luminescence nanodevices ranging from solid-state lasers,[24] flat-panel displays,[25,26] and solar cells[27] to waveguides.[28,29] Besides the potential applications in the fields mentioned above, the upconverting nanomaterials are especially suitable for ultrasensitive multicolor biolabels.[30−32] To our knowledge, hexagonal $NaYF_4$ is one of the most efficient visible UC host materials; however, the rational control of their crystallinity, morphology, and especially epitaxial growth has not been achieved successfully.[33−35] Here we demonstrate the synthesis, DC/UC fluorescence, and self-assembly of the lanthanide-doped $Na(Y_{1.5}Na_{0.5})F_6$ (hexagonal $NaYF_4$) single-crystal nanorods. This facile process should be desirable to other $Na(Ln_{1.5}Na_{0.5})F_6$ systems.

As one of the most efficient visible UC host materials, hexagonal-phase $NaYF_4$ has attracted a great deal of attention over the past two decades.[27,32,33] However, crystalline pure hexagonal $NaYF_4$ was usually obtained with high-temperature disposal technology. However, the high temperature simultaneously caused the wide particle size distribution. Therefore, until now, uniform lanthanide-doped hexagonal $NaYF_4$ single-crystal nanorods with high UC fluorescence and controllable aspect ratios and surface properties have not been attained successfully.[30,33,34] To address this issue, we have adapted our recently reported LSS synthetic strategy[35] to investigate the preparation of lanthanide-doped single-crystal $Na(Y_{1.5}Na_{0.5})F_6$ nanorods. We focused on the preparation of Eu^{3+}- and Tb^{3+}-doped DC nanorods and Yb^{3+}/Er^{3+}- and Yb^{3+}/Tm^{3+}-doped UC nanorods with controllable size. The nanorods were prepared as follows: in a typical nanorod preparation, 20 mL oleic acid, 1.2 g NaOH, 10 mL alcohol, and 4 mL deionized water were mixed together, to which 6.0 mL NaF (1.0 mol/l) aqueous solution and 0.5 mmol (total amounts) of rare-earth nitrate $[Ln(NO_3)_3]$ (Ln: Eu^{3+}, Tb^{3+}, Yb^{3+}/Er^{3+} and Yb^{3+}/Tm^{3+}, grade > 99.99 wt %) aqueous solution (0.1 mol/l, 5.0 mL) were then added under vigorous stirring. The mixture was agitated for another ~20 min and then transferred to a 50 mL autoclave, sealed, and hydrothermal treated at a temperature of 180−205 °C for about 16−24 h. Along with the reaction process of $Na(Y_{1.5}Na_{0.5})F_6$ nanorods, the oleic acid molecules would be coated onto the outer face of the in-situ generated nanorods through the interaction between the rare-earth ions (Ln^{3+}) and carboxyl of the oleic acids with the hydrophobic alkyl chains left outside. For the incompatibility between the hydrophobic alkyl chains on the overlayer of the nanorods and their hydrophilic surrounding and the gravity of the

* Corresponding author. Fax: (+86)10-6278-8765. E-mail: ydli@tsinghua.edu.cn.
† Tsinghua University.
‡ Anhui Normal University.

10.1021/nl060684u CCC: $33.50
Published on Web 07/19/2006

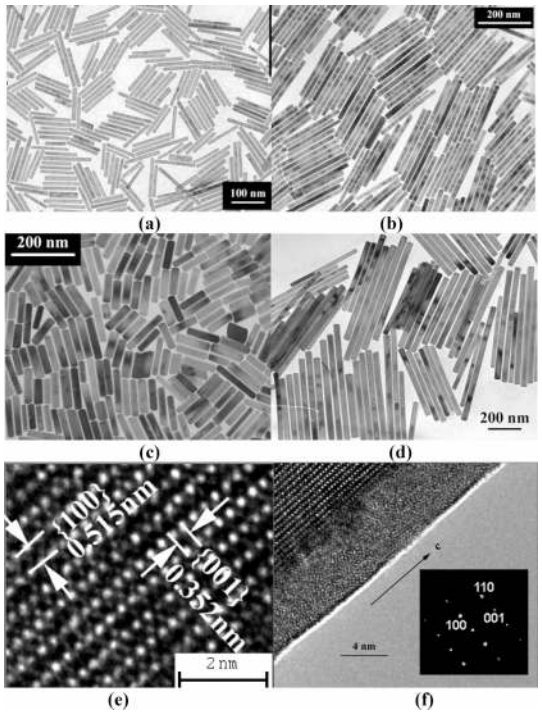

Figure 1. TEM and HRTEM images of the as-prepared rare-earth-doped $Na(Y_{1.5}Na_{0.5})F_6$ nanorods. (a) 25% Eu^{3+} and (b) 5% Eu^{3+}; c and d are doped with 3% Yb^{3+} and 2% Er^{3+}; e and f are the HRTEM images of the single 5% Eu^{3+}-doped $Na(Y_{1.5}Na_{0.5})F_6$ nanorods depicted in b. Reaction temperature: (a) 170 °C for 16 h; (b) 180 °C; (c) 205 °C; (d) 190 °C; (b, c ,and d) for 24 h. The inset of Figure 1f is the electron diffraction pattern of the Fourier transform of HRTEM for the single nanorod. The HRTEM images indicate that the preferred growth direction is along the *c* axis.

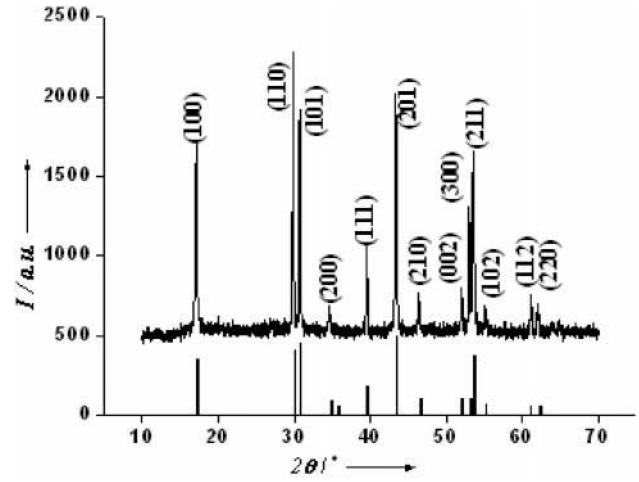

Figure 2. Powder X-ray diffraction pattern of the $Na(Y_{1.5}Na_{0.5})F_6$:Eu^{3+} nanorods purified by water washing to remove the excess NaF. The other lanthanide-doped nanorods have similar XRD patterns and are not depicted here.

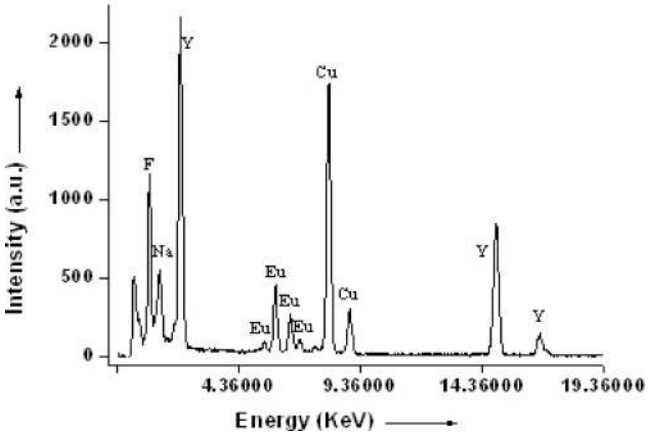

Figure 3. EDXA of the Eu^{3+}-doped $Na(Y_{1.5}Na_{0.5})F_6$ nanorods.

as-prepared nanorods, the nanorods can be collected easily at the bottom of the container. And then the obtained nanorods will be dispersed easily in nonpolar solvent such as cyclohexane and aggregated by adding polar solvent such as ethanol, which enabled their purification and application. All of the chemicals are analytical or higher grade and used without further purification.

Figure 1 shows the typical transmission electron microscopy (TEM) images of the as-synthesized nanorods. These nanorods display uniform morphology and high quality. From these TEM images, it can be seen that the nanorods have self-assembled into nanorafts along with their long axes and then into large-scale ordered 2D patterns on the surface of the TEM grid. As shown in the figure, with the decrease of the dopant concentration of Eu^{3+} from 25% (Figure 1a) to 5% (Figure 1b), the diameters of the $Na(Y_{1.5}Na_{0.5})F_6$:Eu^{3+} nanorods increased from ~15 nm to ~20 nm and the lengths elongated from ~120 nm up to ~220 nm. TEM images of Yb^{3+} (3%)/Er^{3+} (2%) ion-pair codoped nanorods have also been depicted in Figure 1. With a different solvothermal temperature, the aspect ratio of the nanorods was changed from ~5.1 (Figure 1c, 205 °C) to ~22.3 (Figure 1d, 190 °C). The as-prepared nanorods are sensitive to the electron beam in TEM assays. Therefore, it also can be seen that there are many contrasts in single nanorods in TEM images. It is worthy to note that the Tb^{3+}-doped and the Yb^{3+}/Tm^{3+}-codoped nanorods have a similar morphology with high quality (Supporting Information). Typical high-resolution transmission electron microscopy (HRTEM) of the europium (5%)-doped nanorods revealed their highly crystalline nature and structural uniformity (Figure 1e and f). Also, the HRTEM image shows an interplanar spacing of ~0.515 and 0.352 nm corresponding to the ⟨100⟩ and ⟨001⟩ planes of $Na(Y_{1.5}Na_{0.5})F_6$, respectively. The electron diffraction pattern (inset of Figure 1f) from the Fourier transform of HRTEM also demonstrated unambiguously the single-crystalline nature of the sample; it can be readily indexed as hexagonal-phase $Na(Y_{1.5}Na_{0.5})F_6$, consistent with the XRD (ICDD Card No.16-0334) results (Figure 2). From the HRTEM images, it can be seen that the preferred growth direction of the nanorods was along the ⟨001⟩ direction. During the HRTEM measurements, the elemental components of the nanorods were detected by energy-dispersive X-ray analysis (EDAX). All of the EDXA results of different lanthanide-doped nanorods are consistent with their real elemental components, respectively. For an example, we only depicted the EDAX of $Na(Y_{1.5}Na_{0.5})F_6$:Eu nanorods (Figure 3). The EDAX results confirmed that the main elemental components are Na, Y, and F. In addition, a minor doped ion of Eu has also been found; meanwhile, the Eu^{3+} doping concentration in the

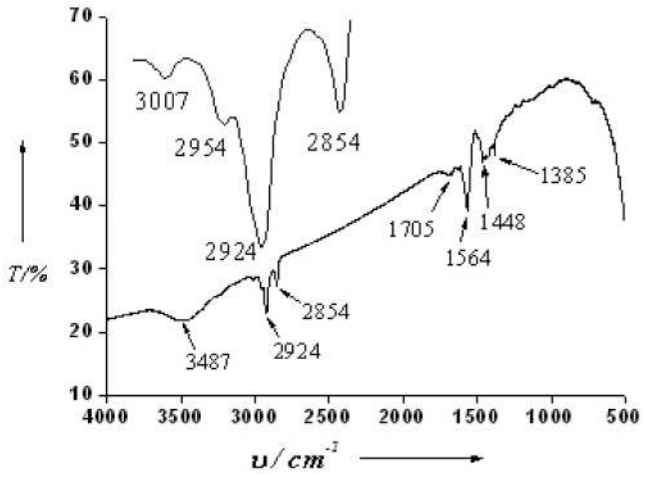

Figure 4. FTIR spectrum of the $Na(Y_{1.5}Na_{0.5})F_6:Eu^{3+}$ nanorods.

nanorods is experimentally determined to be 4.857% by X-ray fluorescence (XRF) analysis. In addition, the surfactant overlayer of the nanorods was identified with Fourier transform infrared (FTIR) studies (Figure 4). As shown in Figure 4, the broad band at 3487 cm^{-1} characterizing mode is appreciable for the O−H (COO−H) stretching vibration. The 2924 and 2854 cm^{-1} transmission bands are assigned to the asymmetric (ν_{as}) and symmetric (ν_s) stretching vibration of methylene (CH_2) in the long alkyl chain of the oleic acid molecule, respectively. Accordingly, the ═C−H stretching peak is located at 3007 cm^{-1} in the FTIR spectrum, and the peak at 1705 cm^{-1} is attributed to the C═O stretching vibration frequency. The bands at 1564 and 1448 cm^{-1} can also be assigned to the asymmetric (ν_{as}) and symmetric (ν_s) stretching vibration of the carboxylic group (−COOH), respectively. Just for the oleic acid overlayer, these as-prepared nanorods are transparently dispersed into nonpolar solvent such as cyclohexane and can be aggregated by adding polar solvent such as ethanol, which enabled their purification and application both in solid and fluid environments.

We have also characterized the luminescent properties of the new lanthanide-doped nanorods. First, the DC fluorescence spectra of the samples with a doping concentration of 5% (Eu^{3+} or Tb^{3+}) were measured carefully (Figure 5). The emission spectrum of $Na(Y_{1.5}Na_{0.5})F_6:Eu^{3+}$ nanorods consists of lines mainly located in the red spectral area with a 265 nm excitation (Figure 5a). Meanwhile, the unexpectedly bright green fluorescence of $Na(Y_{1.5}Na_{0.5})F_6:Tb^{3+}$ nanorods corresponding to the $^5D_4 \rightarrow {}^7F_5$ peak at 543 nm is the dominant emission[36] (excitation wavelength is 220 nm) (Figure 5b). In addition to the main peak, other weak emissions have also been assigned clearly in the figure. The strong DC luminescence inspired us to exploit their potentials for sensitive fluorescence imaging. Figure 5 also depicted the fluorescence imaging photos of $Na(Y_{1.5}Na_{0.5})F_6:Eu^{3+}$ (Figure 5c) and $Na(Y_{1.5}Na_{0.5})F_6:Tb^{3+}$ (Figure 5d) nanorods. All of the results demonstrated here manifest their powerful potentials as DC fluorescent labels.

Besides the DC fluorescence of the Eu^{3+}- and Tb^{3+}-doped $Na(Y_{1.5}Na_{0.5})F_6$ nanorods that were demonstrated, the UC luminescence of Yb^{3+}/Er^{3+} and Yb^{3+}/Tm^{3+} ion-pair codoped nanorods were also investigated in this work. With infrared excitation (~980 nm), the UC fluorescence spectra of $Na(Y_{1.5}Na_{0.5})F_6:Yb^{3+}/Tm^{3+}$ and $Na(Y_{1.5}Na_{0.5})F_6:Yb^{3+}/Er^{3+}$ nanorods are presented in Figure 6. The upconversion luminescence mechanism of both $Na(Y_{1.5}Na_{0.5})F_6:Yb^{3+}/Tm^{3+}$ and $Na(Y_{1.5}Na_{0.5})F_6:Yb^{3+}/Er^{3+}$ nanorods are shown clearly in the

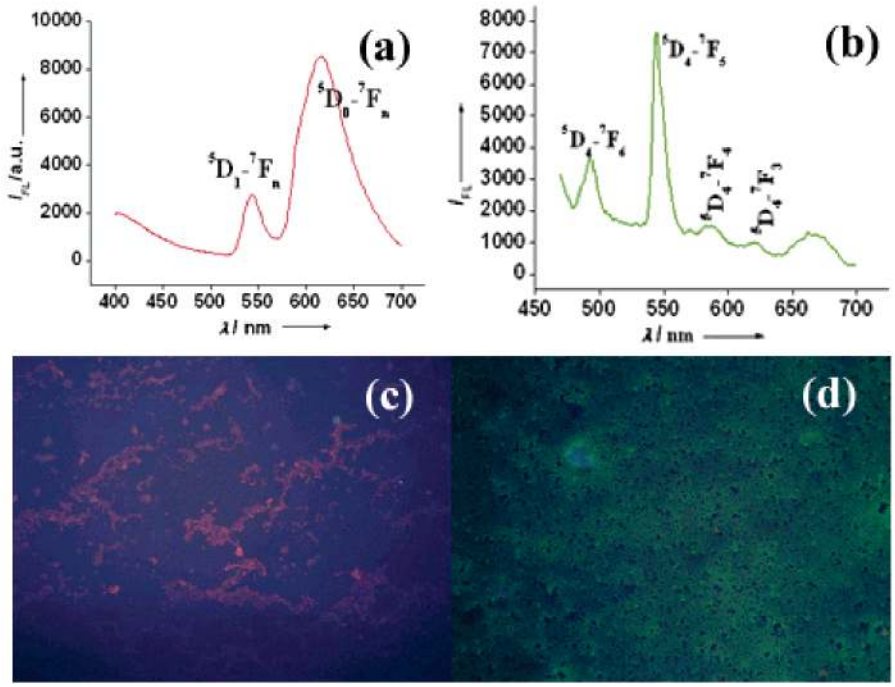

Figure 5. Room-temperature down-conversion fluorescence emission spectra and color luminescence images of the as-synthesized 5% Eu^{3+} (a and c) and 5% Tb^{3+} (b and d) doped $Na(Y_{1.5}Na_{0.5})F_6$ nanorods. The excitation wavelength is 265 and 220 nm to a and b, respectively. The excitation and emission slits of 5.0 nm are used thoroughly.

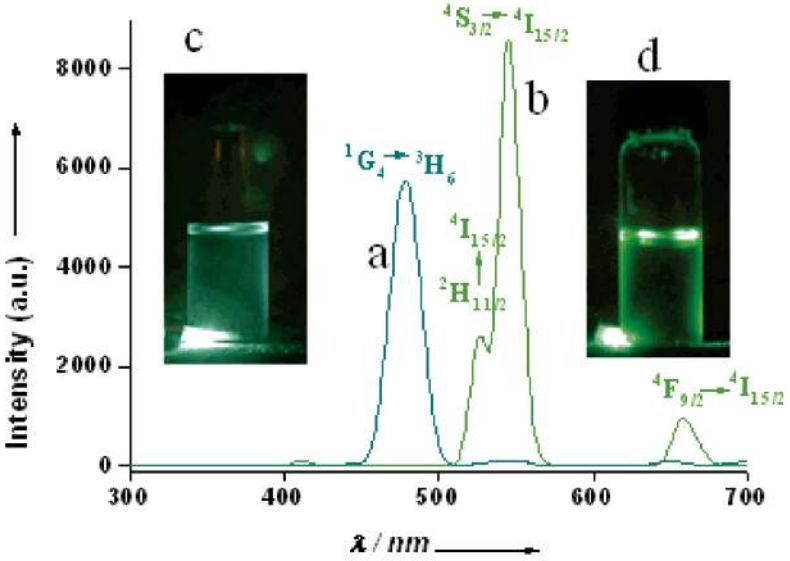

Figure 6. UC fluorescence spectra and eye-visible luminescence photos of the $Na(Y_{1.5}Na_{0.5})F_6:Yb^{3+}/Tm^{3+}$ (a and c) and $Na(Y_{1.5}Na_{0.5})F_6:Yb^{3+}/Er^{3+}$ (b and d) nanorods. The fluorescence spectra are recorded on a F-4500 Hitachi spectrophotometer with an excitation and emission slit of 5.0 nm. UC luminescence photos are recorded with a CCD camera. The excitation source used is a portable 980 nm laser with a 0−800 mW adjustable excitation energy.

schematic energy level diagrams (see Supporting Information Figure S2). The blue luminescence (470 nm) that resulted from the $^1G_4-{}^3H_6$ energy transition of Tm^{3+} ion is the main emission[34] of $Na(Y_{1.5}Na_{0.5})F_6:Yb^{3+}/Tm^{3+}$ nanorods (Figure 6a). The scheme of the upconversion mechanism has shown clearly that the three emissions of $Na(Y_{1.5}Na_{0.5})F_6:Yb^{3+}/Er^{3+}$ nanorods observed are attributed to transitions $^2H_{11/2}-{}^4I_{15/2}$ (~519 nm), $^2S_{3/2}-{}^4I_{15/2}$ (~541 nm), and $^4F_{9/2}-{}^4I_{15/2}$ (~653 nm) for the Er^{3+} ions[32,33] (Figure 6b). Meanwhile, the dominant emission is located at green luminescence range. The eye-visible blue and green UC fluorescence photos of the transparent cyclohexane colloid solution of the Yb^{3+}/Tm^{3+} (Figure 6c) and Yb^{3+}/Tm^{3+} (Figure 6d) codoped nanorods were also depicted. So, both the DC and UC luminescence results powerfully manifested that the as-prepared $Na(Y_{1.5}Na_{0.5})F_6$ nanorod is an excellent luminescence host material.

In conclusion, we have developed a facile synthetic strategy for the highly luminescent DC and UC $Na(Y_{1.5}Na_{0.5})F_6$ nanorods with controllable aspect ratios and surface properties. Their novel DC/UC fluorescence, and controllable morphology and surface might promise further fundamental research and technological application such as nanoscale optoelectronics, solar cells, anticounterfeiting, solid-state lasers, and ultrasensitive biolabels especially in vivo imaging.

Acknowledgment. We express our deep thanks to Prof. Charles M. Lieber of Harvard University for his helpful discussion in the preparation of this work. We also thank the financial support of NSFC (50372030, 90406003) and the State Key Project of Fundamental Research for Nanomaterials and Nanostructures.

Supporting Information Available: Experimental details, schematic energy level diagrams, and TEM images. This material is available free of charge via the Internet at http://pubs.acs.org.

References

(1) Duan, X. F.; Huang, Y.; Agarwal, R.; Lieber, C. M. *Nature* **2003**, *421*, 241−245.
(2) Aldana, J.; Wang, Y. A.; Peng, X. G. *J. Am. Chem. Soc.* **2001**, *123*, 8844−8850.
(3) Wang, X. D.; Summers, C. J.; Wang, Z. L. *Nano Lett.* **2004**, *4*, 423−426.
(4) Law, M.; Sirbuly, D. J.; Johnson, J. C.; Goldberger, J.; Saykally, R. J.; Yang, P. D. *Science* **2004**, *305*, 1269−1273.
(5) Hu, J. T.; Min, O. Y.; Yang, P. D.; Lieber, C. M. *Nature* **1999**, *399*, 48−51.
(6) Cao, J.; Wang, Q.; Dai, H. *Nat. Mater.* **2005**, *4*, 745−749.
(7) Javey, A.; Kim, H.; Brink, M.; Wang, Q.; Ural, A.; Guo, J.; McIntyre, P.; McEuen, P.; Lundstrom, M.; Dai, H. J. *Nat. Mater.* **2002**, *1*, 241−246.
(8) Gudiksen, M. S.; Lauhon, L. J.; Wang, J.; Smith, D. C.; Lieber, C. M. *Nature* **2002**, *415*, 617−620.
(9) Huang, M. H.; Mao, S.; Feick, H.; Yan, H. Q.; Wu, Y. Y.; Kind, H.; Weber, E.; Russo, R.; Yang, P. D. *Science* **2001**, *292*, 1897−1899.
(10) Johnson, J. C.; Choi, H. J.; Knutsen, K. P.; Schaller, R. D.; Yang, P. D.; Saykally, R. J. *Nat. Mater.* **2002**, *1*, 106−110.
(11) Law, M.; Greene, L. E.; Johnson, J. C.; Saykally, R.; Yang, P. D. *Nat. Mater.* **2005**, *4*, 455−459.
(12) Gur, I.; Fromer, N. A.; Geier, M. L.; Alivisatos, A. P. *Science* **2005**, *310*, 462−465.
(13) Huynh, W. U.; Peng, X. G.; Alivisatos, A. P. *Adv. Mater.* **1999**, *11*, 923−927.
(14) Cui, Y.; Wei, Q. Q.; Park, H. K.; Lieber, C. M. *Science* **2001**, *293*, 1289−1292.
(15) Kong, J.; Franklin, N. R.; Zhou, C. W.; Chapline, M. G.; Peng, S.; Cho, K. J.; Dai, H. J. *Science* **2000**, *287*, 622−625.
(16) Barone, P. W.; Baik, S.; Heller, D. A.; Strano, M. S. *Nat. Mater.* **2005**, *4*, 86−92.
(17) Law, M.; Kind, H.; Messer, B.; Kim, F.; Yang, P. D. *Angew. Chem., Int. Ed.* **2002**, *41*, 2405−2408.
(18) Pan, A. L.; Yang, H.; Liu, R. B.; Yu, R. C.; Zou, B. S.; Wang, Z. L. *J. Am. Chem. Soc.* **2005**, *127*, 15692−15693.
(19) Kuykendall, T.; Pauzauskie, P. J.; Zhang, Y. F.; Goldberger, J.; Sirbuly, D.; Denlinger, J.; Yang, P. D. *Nat. Mater.* **2004**, *3*, 524−528.
(20) Goldberger, J.; He, R. R.; Zhang, Y. F.; Lee, S. W.; Yan, H. Q.; Choi, H. J.; Yang, P. D. *Nature* **2003**, *422*, 599−602.
(21) Peng, X. G.; Manna, L.; Yang, W. D.; Wickham, J.; Scher, E.; Kadavanich, A.; Alivisatos, A. P. *Nature* **2000**, *404*, 59−61.

(22) Peng, Z. A.; Peng, X. G. *J. Am. Chem. Soc.* **2001**, *123*, 1389−1395.
(23) Peng, X. G. *Adv. Mater.* **2003**, *15*, 459−463.
(24) Heine, F.; Heumann, E.; Danger, T.; Schweizer, T.; Huber, G.; Chai, B. *Appl. Phys. Lett.* **1994**, *65*, 383−384.
(25) Maciel, G. S.; Biswas, A.; Kapoor, R.; Prasad, P. N. *Appl. Phys. Lett.* **2000**, *76*, 1978−1980.
(26) Downing, E.; Hesselink, L.; Ralston, J.; Macfarlane, R. *Science* **1996**, *273*, 1185−1189.
(27) Shalav, A.; Richards, B. S.; Trupke, T.; Kramer, K. W.; Gudel, H. U. *Appl. Phys. Lett.* **2005**, *86*, 13503−13505.
(28) Strohhofer, C.; Polman, A. *J. Appl. Phys.* **2001**, *90*, 4314−4320.
(29) Kik, P. G.; Polman, A. *J. Appl. Phys.* **2003**, *93*, 5008−5012.
(30) Yi, G. S.; Lu, H. C.; Zhao, S. Y.; Yue, G.; Yang, W. J.; Chen, D. P.; Guo, L. H. *Nano Lett.* **2004**, *4*, 2191−2196.
(31) van de Rijke, F.; Zijlmans, H.; Li, S.; Vail, T.; Raap, A. K.; Niedbala, R. S.; Tanke, H. J. *Nat. Biotechnol.* **2001**, *19*, 273−276.
(32) Wang, L. Y.; Yan, R. X.; Hao, Z. Y.; Wang, L.; Zeng, J. H.; Bao, J.; Wang, X.; Peng, Q.; Li, Y. D. *Angew. Chem., Int. Ed.* **2005**, *44*, 6054−6057.
(33) Zeng, J. H.; Su, J.; Li, Z. H.; Yan, R. X.; Li, Y. D. *Adv. Mater.* **2005**, *17*, 2119−2123.
(34) Heer, S.; Kompe, K.; Gudel, H. U.; Haase, M. *Adv. Mater.* **2004**, *16*, 2102−2104.
(35) Wang, X.; Zhuang, J.; Peng, Q.; Li, Y. D. *Nature* **2005**, *437*, 121−124.
(36) Yan, R. X.; Li, Y. D. *Adv. Funct. Mater.* **2005**, *15*, 763−770.

NL060684U

Supporting Information

$Na(Y_{1.5}Na_{0.5})F_6$ Single-Crystal Nanorods as Multicolor Luminescent Materials

Leyu Wang and Yadong Li

Experimental Section

In a typical nanorod preparation, 20 ml oleic acid, 1.2 g NaOH, 10 ml alcohol, 4 ml deionized water were mixed together, to which 6.0-8.0 ml NaF (1.0 mol/l) aqueous solution and 0.5 mmol (total amounts) of rare-earth nitrate [$Ln(NO)_3$] aqueous solution (0.5 mol/l, 1.0 ml) were then added under vigorous stirring. The mixture was agitated for another ~20 min, and then transferred to a 50 ml autoclave, sealed and hydrothermal treated at designed temperature of 170 ~ 205 ^oC for about 16-24 hr. Along with the reaction process of $Na(Y_{1.5}Na_{0.5})F_6$ nanorods, the oleic acid molecules would be coated onto the outerface of the in-situ generated nanorods through the interaction between the rare-earth ions (Ln^{3+}) and carboxyl of the oleic acids with the hydrophobic alkyl chains left outside. For the incompatibility between the hydrophobic alkyl chains on the overlayer of the nanorods and their hydrophilic surrounding and the gravity of the as-prepared nanorods, the nanorods can be easily collected at the bottom of the container. And then the obtained nanorods will be easily dispersed in nonpolar solvent such as cyclohexane and aggregated by adding polar solvent such as ethanol, which enabled their purification and application. All the chemicals are analytical or higher grade and used for available without further purification.

The crystal size and morphology of the products were examined with a JEOL JEM-1200EX transmission electron microscope with a tungsten filament at an accelerating voltage of 120 kV. Samples were prepared by placing a drop of a dilute cyclohexane dispersion of nanorods on the surface of a copper grid. High-resolution structural information on the as-prepared nanorods was obtained by high-resolution transmission electron microscopy (HRTEM) on a JEOL JEM-2010F transmission electron microscope operated at 200 kV. Energy dispersive X-ray analysis (EDAX) of

the $Na(Y_{1.5}Na_{0.5})F_6$ nanorods was also performed on the samples during the HRTEM measurements. XRD was carried out to determine the nature of the materials whether it is amorphous or crystalline. In this work, XRD were carried out using a Rigaku D255OPC X-ray diffractometer which employs Cu-Kα radiation of wavelength λ=1.5418Å. The operation voltage and current were kept at 40 kV and 40 mA, respectively. A 2θ range from 10 to 70° was covered in steps of 0.02° with a count time of 2s. FTIR spectra were conducted with a Nicolet 560 Fourier-transform infrared spectrophotometer.

Fluorescence imaging experiment was conducted and the color images were directly obtained with an epifluorescence microscope (Olympus□BX51) that was equipped with a high-resolution CCD camera (6.4 million pixels) (Olympus-Z5050) and a 100-W Hg excitation lamp. Samples of dilute nanorods were deposited and spread on glass coverslips, resulting in dispersive nanorod layer on the surface. The optical properties of europium and terbium doped nanorods were characterized through their photoluminescence (Hitachi F-4500 fluorescence spectrophotometer operated at room temperature with a 150-W continuous-wave xenon lamp). Upconversion luminescence spectra were recorded on a Hitachi F-4500 fluorescence spectrophotometer with a 0-800 mW adjustable laser (980 nm Beijing Hi-Tech Optoelectronic Co., China) as the excitation source, instead of the xenon source in the spectrophotometer, and with a fiber optic accessory. The eye-visible upconversion luminescence photo was acquired under the same exciting conditions with the same potable laser.

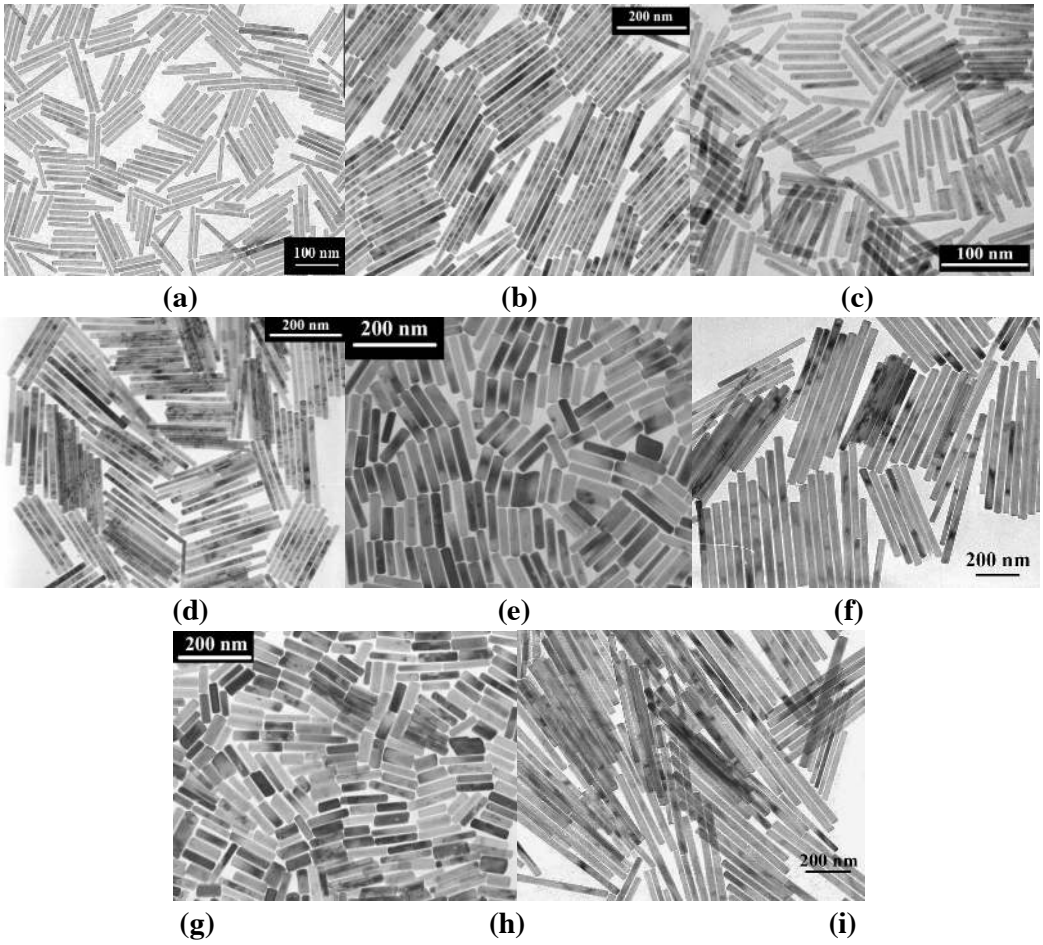

Figure S1. TEM images of the as-prepared rare-earth doped $Na(Y_{1.5}Na_{0.5})F_6$ nanorods. a) 25% Eu^{3+} and b) 5% Eu^{3+}; c) 25% Tb^{3+} and d) 5% Tb^{3+}; e) and f) are doped with 3% Yb^{3+} and 2% Er^{3+}; g) and h) are doped with 3% Yb^{3+} and 2% Tm^{3+}; Reaction temperature and time: a and c, 170 ^{o}C for 16 hr; b and d, 180 ^{o}C for 24 hr; e and g, 205 ^{o}C for 24 hr; f and h, 190 ^{o}C for 24 hr.

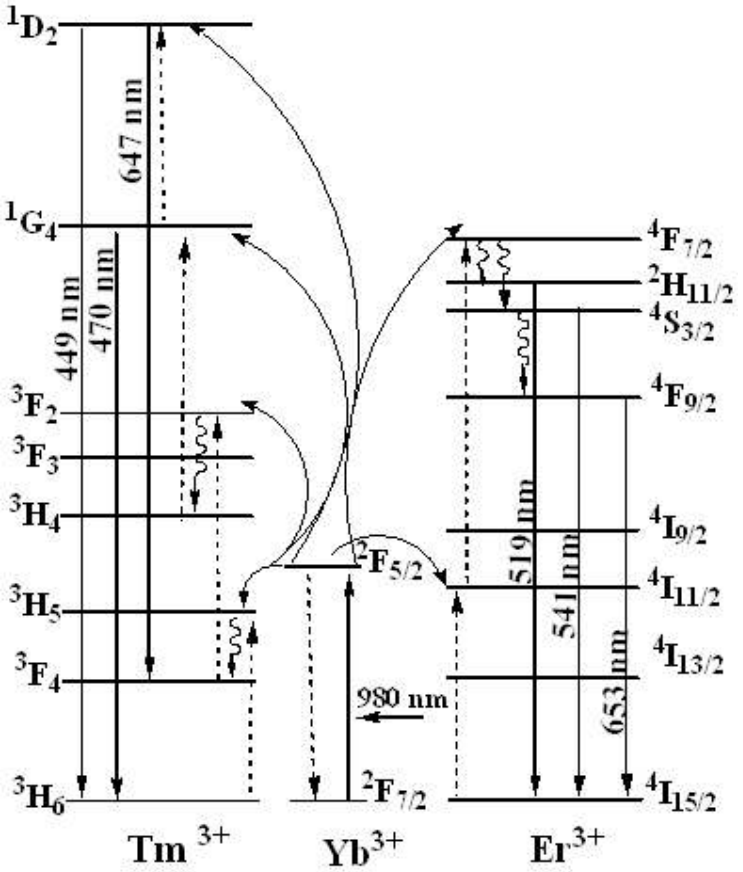

Figure S2. Schematic energy level diagrams of upconversion excitation and visible emission for the Yb^{3+}–Tm^{3+} and Yb^{3+}–Er^{3+} systems.